Pergamon

SCIENCE DIRECT®

Bioorganic & Medicinal Chemistry Letters 13 (2003) 107–110

BIOORGANIC & MEDICINAL CHEMISTRY LETTERS

Design of Novel *N*-(2,4-Dioxo-1,2,3,4-tetrahydro-thieno[3,2-*d*]pyrimidin-7-yl)-guanidines as Thymidine Phosphorylase Inhibitors, and Flexible Docking to a Homology Model

Melissa L. P. Price,[a,*] Wayne C. Guida,[b,c] Tara E. Jackson,[b] Jason A. Nydick,[b] Patricia L. Gladstone,[a] José C. Juarez,[a] Fernando Doñate[a] and Robert J. Ternansky[a]

[a]*Attenuon, L.L.C., San Diego, CA 92121, USA*
[b]*Department of Chemistry, Eckerd College, St. Petersburg, FL 33711, USA*
[c]*Drug Discovery Program, H. Lee Moffitt Cancer Center and Research Institute at the University of South Florida, Tampa, FL 33612, USA*

Received 22 May 2002; accepted 24 September 2002

Abstract—A novel class of thymidine phosphorylase (TP) inhibitors has been designed based on analogy to the enzyme substrate as well as known inhibitors. Flexible docking studies, using a homology model of human TP, of the designed *N*-(2,4-dioxo-1,2,3,4-tetrahydro-thieno[3,2-*d*]pyrimidin-7-yl)-guanidines as well as their synthetic precursors provide insight into the observed experimental trends in binding affinity.

Thymidine phosphorylase (TP) catalyzes the reversible phosphorolysis of thymidine (**1**) to thymine and 2-deoxyribose-1-phosphate (Scheme 1).[1,2] By analogy to purine nucleoside phosphorylase,[3] the reaction likely proceeds through an oxocarbenium ion-like transition state. The phosphorylated sugar product is further converted to 2-deoxy-D-ribose which has been shown to have chemotactic activity in vitro and angiogenic activity in vivo.[4] Therefore, inhibitors of TP may find utility as suppressors of tumor growth.[5]

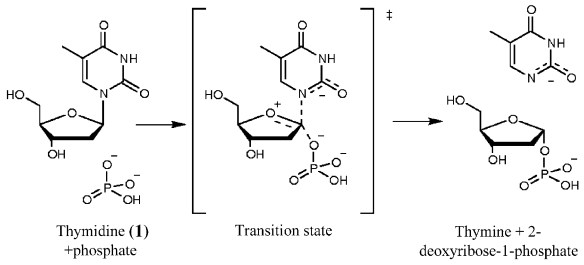

Scheme 1.

Taiho Pharmaceutical Co. has reported the most potent TP inhibitor to date, 5-chloro-6-(2-iminopyrrolidin-1-yl)methyl-2,4(1*H*,3*H*)-pyrimidinedione hydrochloride (**2**) which inhibits human TP with an IC_{50} value of 35 nM.[6] Our designed thienopyrimidinyl guanidines, **3** and **4**, preserve the interactions of the pyrimidine ring in **1** and **2**, substitute an isosteric sulfur atom for the chlorine atom in **2**, and maintain the positive-charge character of the iminopyrrolidine in **2**, which like **2,** may mimic the oxocarbenium ion-like transition state in thymidine phosphorolysis.

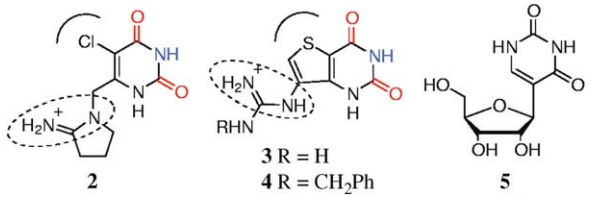

Pyrimidine nucleoside phosphorylase (PyNP) (42% sequence identity using Clustalw[7] for alignment against the human sequence) catalyzes the same reaction as TP, as well as the conversion of uridine to uracil. Unlike other structures of TP,[8,9] the high-resolution

*Corresponding author. Fax: +1-858-622-0517; e-mail: price@attenuon.com

0960-894X/03/$ - see front matter © 2002 Published by Elsevier Science Ltd.
PII: S0960-894X(02)00828-4

X-ray structure of PyNP, co-crystallized with pseudouridine (**5**), shows both an open (inactive) conformation and a closed (presumed active) conformation of the enzyme.[10] Using these coordinates, we have built a homology model of human TP (HuTP). While others have built a homology model of HuTP in the open conformation based on the X-ray structure of *Escherichia coli* TP,[11] to our knowledge this is the first model that depicts the enzyme in the active conformation. Flexible docking of the compounds **1**–**5** and the synthetic precursors **12**–**14** using the homology model provide insight into the observed experimental trends in binding affinity.

Structural coordinates for PyNP co-crystallized with **5** (pdb entry: 1brw, chain A)[10] were obtained from the RCSB Protein Data Bank.[12] The sequence of HuTP was obtained from the SwissProt database[13] and Swiss-Model was used to construct the homology model.[14] Crystallographic waters were not included in the homology model. The model was refined via restrained energy minimization using the MacroModel/BatchMin software.[15] The AMBER* force field was employed using a distance-dependent dielectric of 4*r*. Successive, restrained, energy minimizations were performed using a harmonic restraining potential on each atom starting with a restraining force constant of 500 kJ/mol Å^2. This force constant was decreased by a factor of ca. 2 until the final energy minimization was unconstrained.

The same force field and dielectric was also used in all of the flexible docking simulations with the exception that ligand charges were fit to the electrostatic potential from ab initio calculations at the HF/6-31G* level using Jaguar.[16] The protein was truncated to a ca. 15 Å shell from any ligand atom in **4**. The protein side chains for twenty residues were fully flexible; the backbone atoms of these residues were constrained with a force constant of 100 kJ/mol Å^2. All other residues were frozen at their initial positions and thus only their nonbonded potential energy contributed to the overall potential. Restricting the conformational freedom of residues beyond the first shell of interaction with the ligand provides a necessary balance between docking accuracy and simulation time. Each flexible docking simulation consisted of 20,000 steps of the LMOD docking search procedure,[17,18] which performs orientational as well as conformational sampling, using Batchmin.[15] In order to validate the LMOD method, **5** was docked into PyNP (closed conformation) starting with an arbitrary orientation and conformation for the ligand. The global minimum had an rmsd of 1.09 Å for the uracil ring atoms. Comparison of the ribose was not possible since this part of the electron density was ill-defined in the crystal structure.

The unsubstituted guanidines **3** and **14** were synthesized as shown in Scheme 2. The nitro thiophene regioisomers **6** and **7** were prepared and separated according to the procedure described by Elliott et al.[19] The acetyl groups were removed with HCl in methanol, and the resulting free amines were treated with ethyl isocyanatoformate to afford **8** and **9**. Reduction of the nitro groups with iron in refluxing acetic acid/ethanol gave amines **10** and **11**,[20] which cyclized with sodium methoxide in methanol to provide thieno-pyrimidine diones **12** and **13**.[21] The desired guanidine salts **3** and **14** were obtained by treating **12** and **13**, respectively, with cyanamide in acetic acid at 110 °C.

Benzyl guanidine **4** was prepared starting from benzyl amine, which was converted to the corresponding cyanamide **15** with cyanogen bromide and sodium bicarbonate in methanol. Thienopyrimidine dione **12** and **15** in hexafluoroisopropanol were heated at 110 °C in a sealed tube for 65 h,[22] and guanidine **4** was separated from the crude reaction mixture by preparative HPLC (Scheme 3).

The quality of our HuTP homology model was examined with ProCheck.[23] For the 20 Å shell of residues surrounding the binding site, 89.0% of the ϕ and ψ angles fell into the most favorable region of the Ramachandran map and 10.4% were in the additionally-allowed region. Furthermore, χ1 and χ2 angles were found to have fewer eclipsed conformations than a typical 2 Å resolution structure. Finally, the analysis provided an overall g-factor of 0.1 for our model, where a g-factor is a measure of the conformational violations

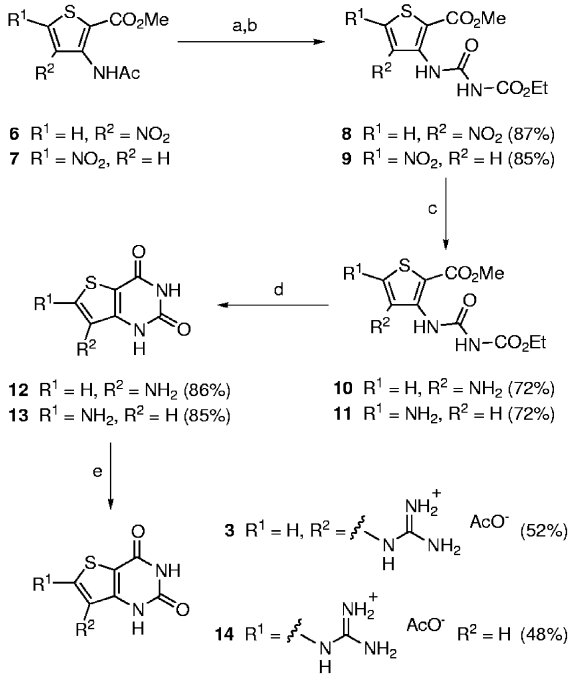

Scheme 2. (a) HCl (concd), MeOH, Δ; (b) ethyl isocyanatoformate, $CHCl_3$, Δ; (c) Fe(s), AcOH, EtOH, Δ; (d) NaOMe, MeOH, Δ; (e) cyanamide, AcOH, Δ.

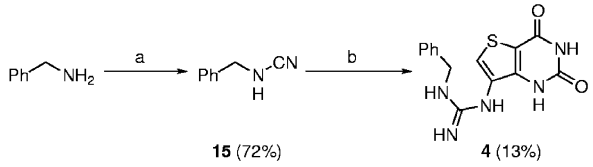

Scheme 3. (a) Cyanogen bromide, $NaHCO_3$, MeOH, 0 °C; (b) **12**, HFIP, 100 °C.

present. For reference, a g-factor of −0.4 is expected for a crystal structure of 2 Å resolution, and more positive g-factors would be expected for higher resolution models. Figure 1 shows a ribbon-type diagram of the C_{alpha} superimposition of the HuTP model and PyNP.

In addition to having comparable backbone geometries, we expect that the arrangement of the conserved residues in the binding site should be maintained between the two proteins. To ensure that the model-building process did not distort this expected arrangement, we docked **5** into both PyNP and HuTP and compared the relative positioning of these residues. Figure 2 shows the overlay of the sidechains; all of the intermolecular hydrogen bonds in PyNP are maintained in the HuTP model as well.

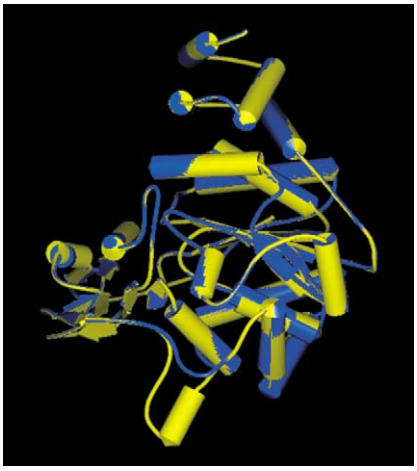

Figure 1. Structural comparison of PyNP[10] (blue) and HuTP (yellow) homology model.

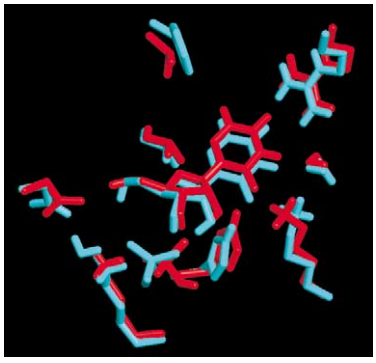

Figure 2. Comparison of the PyNP (cyan) and HuTP (red) binding sites when complexed with **5**.

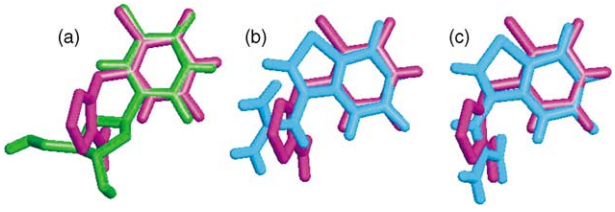

Figure 3. Docked conformations of (a) **1** (green) and **2** (purple) and (b)–(c) **2** (purple) and **3** (cyan). (a) and (b) show global minimum conformations; (c) illustrates another low-energy structure for **3**. The protein has been removed for clarity.

The global minimum conformations from docking of **1** versus **2** (Fig. 3a) and **2** versus **3** (Fig. 3b) are illustrated below. The proximity of the endocyclic nitrogen atom in the iminopyrrolidine of **2** to the C4′ ribose oxygen atom in **1** supports the hypothesis that **2** confers inhibition by transition-state mimicry (Fig. 3a). Furthermore, the similar binding orientation of **3** suggests that this compound may also resemble the transition state electronically (Fig. 3b and c). In fact, an additional low-energy docked conformation of **3**, which is ca. 1.5 kcal/mol higher in energy than the global minimum, shows excellent overlay with **2** (Fig. 3c). It is unclear to what extent these two conformations are actually populated, considering that 1.5 kcal/mol is probably within the inherent error in using a homology model and a force field that did not include these ligands in the parameterization set.

As shown in Table 1, compound **3** has a significantly lower binding affinity compared to **2**. While other active 'purine-like' TP inhibitors have been previously repor-

Table 1. Experimental binding affinities[a]

Compd	K_I (μM)[b]
1	—
2	0.005 (±0.003)
3	76.0 (±6.4)
4	64.3 (±1.0)
5	na[c]
12	>600[d]
13	>300[d]
14	>2400[d]

[a]The enzyme assay was performed with recombinant TP as reported by Wataya[24] with the exception that arsenate was substituted for phosphate to reduce the reversibility of the reaction.
[b]Values represent the mean of at least three experiments (standard deviations in parentheses).
[c]na, not available.
[d]Low solubility prevented accurate determination of the binding affinity.

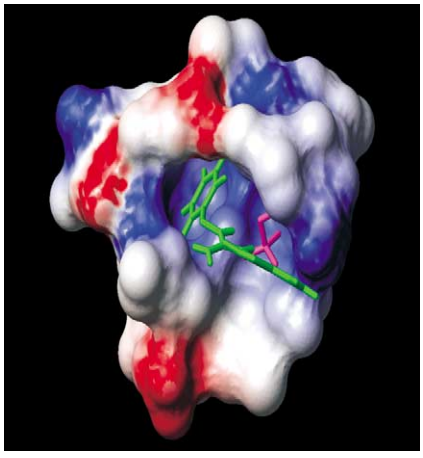

Figure 4. Electrostatic potential surface of the HuTP binding pocket occupied by the benzyl subtituent in **4** (green). Phosphate is shown in purple.

ted,[25,26] the bulkier thiophene ring warrants consideration that sterics may play a role in the reduced affinity. However, calculations of the van der Waals contributions to the intermolecular interaction energies of the docked complexes (data not shown) refute this suggestion. Estimates of the relative solvation free energies for binding ($\Delta\Delta G_{solvation}$) of **2** and **3** were then obtained by reducing the solvation energy of the complex by that of the unbound protein and ligand (single-point calculations using the GB/SA solvation model);[27] the $\Delta\Delta G_{solvation}$ for **3** is larger than **2** by ca. 9 kcal/mol. While the magnitude of these relative solvation free energies may be overestimated, these results indicate that there is an enhanced desolvation penalty for the more hydrophilic guanidine which is likely a dominant contributor to the reduced affinity of **3** compared to **2**. Although the amino compounds **12** and **13** suffer less from this solvation penalty than **3**, there is a >10 kcal/mol loss of favorable intermolecular interactions in the binding site.

It is worth noting that the bulkier **4** maintains a similar level of activity to the unsubstituted **3**. Our docking studies indicate that space is available in the binding site for the extra aromatic ring, and that the electrostatic potential in this region is positively charged, as shown in Figure 4. Attempting to modulate the activity of the compound, by functionalizing the benzene ring or exploring other aromatic substituents, is a promising direction for future work. Another attractive approach for enhancing binding affinity is functionalization at the 6-position on the thiophene ring which should preorganize the conformation that best mimics the transition state.

In summary, we have designed a novel class of TP inhibitors based on the structural features of known inhibitors and on the mechanism of catalysis. We have also built the first homology model of human TP in the active conformation, and have performed flexible docking studies using this model in order to analyze the details of ligand binding. In addition, these results help rationalize the experimental binding affinities and will assist further lead optimization studies. Finally, this novel class of 'purine-like' compounds may find utility as nucleoside mimics with inhibitory activity against other therapeutic targets.

Acknowledgements

We thank Professor Steve Ealick of Cornell University for numerous helpful discussions.

References and Notes

1. Iltzsch, M. H.; el Kouni, M. H.; Cha, S. *Biochemistry* **1985**, *24*, 6799.
2. Friedkin, M.; Roberts, D. *J. Biol. Chem.* **1954**, *207*, 245.
3. Kline, P. C.; Schramm, V. L. *Biochemistry* **1995**, *34*, 1153.
4. Haraguchi, M.; Miyadera, K.; Uemura, K.; Sumizawa, T.; Furukawa, T.; Yamada, Y.; Akiyama, S. *Nature* **1994**, *368*, 198.
5. Matsushita, S.; Nitanda, T.; Furukawa, T.; Sumizawa, T.; Tani, A.; Nishimoto, K.; Akiba, S.; Miyadera, K.; Fukushima, M.; Yamada, Y.; Yoshida, H.; Kanzaki, T.; Akiyama, S. *Cancer Res.* **1999**, *59*, 1911.
6. Fukushima, M.; Suzuki, N.; Emura, T.; Yano, S.; Kazuno, H.; Tada, Y.; Yamada, Y.; Asao, T. *Biochem. Pharmacol.* **2000**, *59*, 1227.
7. Thompson, J. D.; Higgins, D. G.; Gibson, T. *J. Nucleic Acids Res.* **1994**, *22*, 4673.
8. Spraggon, G.; Stuart, D.; Ponting, C.; Finnis, C.; Sleep, D.; Jones, Y. *J. Mol. Biol.* **1993**, *234*, 879.
9. Walter, M. R.; Cook, W. J.; Cole, L. B.; Short, S. A.; Koszalka, G. W.; Krenitsky, T. A.; Ealick, S. E. *J. Biol. Chem.* **1990**, *265*, 14016.
10. Pugmire, M. J.; Ealick, S. E. *Structure* **1998**, *6*, 1467.
11. Cole, C.; Marks, D. S.; Jaffar, M.; Stratford, I. J.; Douglas, K. T.; Freeman, S. *Anti-Cancer Drug Des.* **1999**, *14*, 411.
12. Berman, H. M.; Westbrook, J.; Feng, Z.; Gilliland, G.; Bhat, T. N.; Weissig, H.; Shindyalov, I. N.; Bourne, P. E. *Nucleic Acids Res.* **2000**, *28*, 235.
13. Bairoch, A.; Apweiler, R. *Nucleic Acids Res.* **2000**, *28*, 45.
14. SwissModel, 2002. (http://www.expasy.org/swissmod/SWISS-MODEL.html).
15. Mohamadi, F.; Richards, N. G. J.; Guida, W. C.; Liskamp, R.; Lipton, M.; Caufield, C.; Chang, G.; Hendrickson, T.; Still, W. C. *J. Comput. Chem.* **1990**, *11*, 440.
16. *Jaguar, Ver. 4.0*. Schrodinger: Portland, OR, 2000.
17. Kolossváry, I.; Guida, W. C. *J. Am. Chem. Soc.* **1996**, *118*, 5011.
18. Kolossváry, I.; Guida, W. C. *J. Comput. Chem.* **1999**, *20*, 1671.
19. Elliott, R. L.; O'Hanlon, P. J.; Rogers, N. H. *Tetrahedron* **1987**, *43*, 3295.
20. Jarvest, R. L.; Connor, S. C.; Gorniak, J. G.; Jennings, L. J.; Serafinowska, H. T.; West, A. *Bioorg. Med. Chem. Lett.* **1997**, *7*, 1733.
21. Stanovnik, B.; Tisler, M. *Synthesis* **1972**, 308.
22. Snider, B. B.; O'Hare, S. M. *Tetrahedron Lett.* **2001**, *42*, 2455.
23. Laskowski, R. A.; MacArthur, M. W.; Moss, D. S.; Thornton, J. M. *J. Appl. Cryst.* **1993**, *26*, 283.
24. Wataya, Y.; Santi, D. W. *Anal. Biochem.* **1981**, *112*, 96.
25. Hirota, K.; Sawada, M.; Sajiki, H.; Sako, M. *Nucleic Acids Symposium Series* **1997**, *37*, 59.
26. Balzarini, J.; Gamboa, A. E.; Esnouf, R.; Liekens, S.; Neyts, J.; De Clercq, E.; Camarasa, M. J.; Perez-Perez, M. J. *FEBS Lett.* **1998**, *438*, 91.
27. Still, W. C.; Tempczyk, A.; Hawley, R. C.; Hendrickson, T. *J. Am. Chem. Soc.* **1990**, *112*, 6127.